



# Effects of input physics on the collapse condition of the oxygen-neon-magnesium core

S.-C. Leung and K. Nomoto

Kavli Institute for the Physics and Mathematics of the Universe (WPI), The University of Tokyo  
Institutes for Advanced Study, The University of Tokyo, Kashiwa, Chiba 277-8583, Japan  
e-mail: shingchi.leung@ipmu.jp

**Abstract.** The evolution of a 8 - 10 solar mass main-sequence star leaves an oxygen-neon-magnesium (ONeMg) core close to the Chandrasekhar mass with a central density about  $10^{9.95}$  g cm<sup>-3</sup>. The consequent electron capture of <sup>16</sup>O and <sup>20</sup>Ne in the core triggers the oxygen-neon deflagration. It has been shown that the collapse criteria is sensitive to the choice of input physics, in particular the flame physics. In this article we study the oxygen deflagration by two-dimensional simulations of an ONeMg core using the turbulent deflagration model. We consider stellar models with different input physics, including the initial flame structure, central density and relativistic effects. We found that in general collapse occurs in most models with a central density above  $10^{9.90}$  g cm<sup>-3</sup>. Also, the initial ignited mass affects the collapse density strongly. On the other hand, the collapse condition does not vary strongly with the inclusion of relativistic effects. Our results suggest that the low mass neutron stars observed in binary pulsars are likely to be produced by the collapse of the ONeMg core left behind by AGB stars. Furthermore, an accurate modelling from stellar evolution is essential for an accurate prediction of the ONeMg core final fate.

**Key words.** AGB stars – Electron Capture Supernovae – Hydrodynamics – turbulent deflagration

## 1. Introduction

It is unclear whether the oxygen-neon deflagration is responsible for the weak explosion as observed in typical Type Ia supernovae, or the direct collapse to form neutron star. In Nomoto & Kondo (1991), the evolution of an ONeMg cores by one-dimensional model with a central density  $10^{9.95}$  g cm<sup>-3</sup> is studied (Miyaji & Nomoto, 1987; Hashimoto et al., 1993). (Note if semi-convective mixing takes place, the ignition density is higher.) It is shown that whether the core collapses into a neutron star depends strongly on the flame properties. This indicates

the importance of multi-dimensional modeling for a consistent approach in modeling flame. In Jones et al. (2016) it is further demonstrated by the first multi-dimensional simulations that the choice of microphysics can influence the explosion strength. Since these ONeMg cores can be the potential candidates of the low mass neutron stars (Schwab et al., 2010) and explain the occurrence rate of the low-mass binary pulsars, a comprehensive understanding in the potential effects of input physics becomes important. In this article, we cover further other important input physics which remain unexplored in the literature. These components are cho-

sen because they are not well constrained by stellar evolution models. They include the central density of the ONeMg core, flame structure and the general relativistic effect.

## 2. Methods

We use our two-dimensional hydrodynamics code which is designed for the explosion phase of supernovae. It has been used to study the nucleosynthesis of Type Ia supernovae using the turbulent deflagration model with delayed detonation transition (Leung & Nomoto, 2017). The code has also been applied to study sub-luminous Type Ia supernovae (Leung et al., 2015a). We refer the interested readers to the instrument paper for the technical details (Leung et al., 2015b). Here we briefly outline the code structure, input physics to model the ONeMg core.

The hydrodynamics code solves the Euler equations in two-dimension in cylindrical coordinates. The spatial discretization is treated by fifth-order weighted essential non-oscillatory (WENO) scheme (Barth & Deconinck, 1999) and the time discretization is treated by third-order five-step non-strong stability preserving Rung-Kutta scheme (Wang & Spiteri, 2007). We use the helmholtz equation of states (Timmes & Arnett, 1999), which includes the electron gas at arbitrary relativistic and degenerate level, ions as an classical gas, photon gas with Planck distribution and electron-positron pair. To follow the chemical composition, we trace the evolution of 7 isotopes, including  $^4\text{He}$ ,  $^{12}\text{C}$ ,  $^{16}\text{O}$ ,  $^{20}\text{Ne}$ ,  $^{24}\text{Mg}$ ,  $^{28}\text{Si}$  and  $^{56}\text{Ni}$ .

We use the level-set method (Reinecke et al., 1999b) to track the propagation of deflagration. For the turbulent flame, we use the speed formula given in Pocheau (1994); Schmidt et al. (2006) with the laminar flame speed obtained from the formula derived in Timmes & Woosley (1992). We use the one-equation model (Clement, 1994; Niemeyer et al., 1995) to trace the production and dissipation of eddy motion in the sub-grid scale. The production by fluid shear motion and dissipation by turbulent expansion, eddy dissipation, diffusion terms and the production by

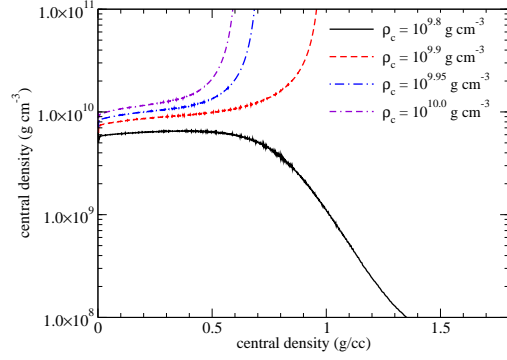


**Fig. 1.** The time evolution of the central density of two models. The exploding (collapsing) model has a central density  $\rho_{c \text{ (ini)}}$  of  $10^{9.8}$ ,  $10^{9.9}$ ,  $10^{9.95}$  and  $10^{10.0}$   $\text{g cm}^{-3}$  respectively. Both models are set with a central ignition kernel of mass and the relativistic effects are ignored.

Rayleigh-Taylor instabilities (Schmidt et al., 2006) are included as turbulence source terms.

To couple with the relativistic effects, we modify the gravity source term following Kim et al. (2012) based on the Tolman-Oppenheimer-Volstoff equations, where the gravitational potential  $\Phi$  satisfies

$$\nabla^2 \Phi = 4\pi G(\rho h \tilde{v} + 2p), \quad (1)$$

where  $\rho$ ,  $p$  are the local mass density and pressure,  $h = 1 + \epsilon + p/\rho$  is the specific enthalpy and  $\tilde{v} = (1 + v)/(1 - v)$ , where  $\epsilon$  and  $v$  are the specific internal energy and velocity.

## 3. Results

We carry out the hydrodynamics simulations of the ONeMg core with oxygen-neon deflagration. In Fig. 1 we plot the central density of two contrasting types of models where one explodes and the other collapses. The initial central density is an important parameter that influences the collapse condition. A slight jump of the central density from  $10^{9.8}$  to  $10^{9.9}$   $\text{g cm}^{-3}$  can make the ONeMg core collapse instead of an explosion. This shows that an accurate prediction of the runaway moment is important to determine the final fate. It influences the electron capture rate, and hence the softening of the ash.

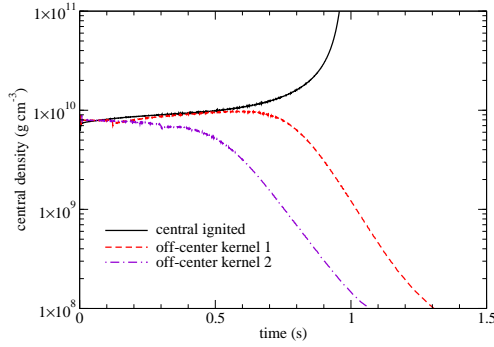


**Fig. 2.** Same as 1, but for the different initial flame configurations. All models are fixed at  $\rho_{c(\text{ini})} = 10^{9.95} \text{ g cm}^{-3}$ .

In Fig. 2 we plot the central density evolution for the same central density at  $10^{9.95} \text{ g cm}^{-3}$  but with different initial flame kernel. The model with a central ignition collapse directly while those with an off-center ignition kernel explode. This means the pre-runaway convection structure in the ONeMg core, which can influence the transport of heat as well as the motion of runaway spot prior to its runaway.

In Fig. 3 we plot the central density evolution for the same central density at  $10^{9.95} \text{ g cm}^{-3}$  but with different initial flame size. All models begin with the central ignition kernel. The model with an initial ash mass  $M_{\text{burn}} \sim 10^{-2} M_{\odot}$  explodes while those with smaller ash masses collapse. This shows that the initial runaway size owing to gamma heating by electron capture is important. It influences the initial propagation of flame, and hence the energy production rate.

In Figure 4 we plot the central density for the models with central flame of burnt mass  $8.56 \times 10^{-4} M_{\odot}$  and with initial central densities  $10^{10.0}$  and  $10^{10.2} \text{ g cm}^{-3}$  respectively. Models with and without relativistic effect corrections are included for comparison. In both cases a direct collapse is observed. The evolution of the central density is not sensitive to the general relativistic corrections to the gravitational potential. The two curves are overlapping each other for both pairs of models at all time.

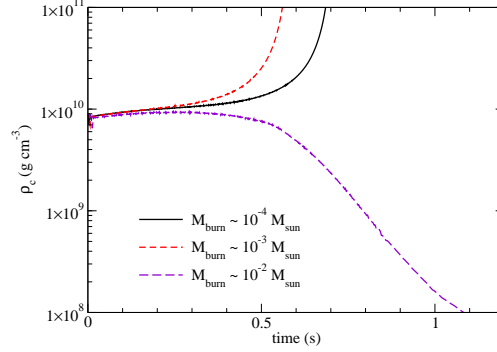


**Fig. 3.** Same as 1, but for different flame size. All models are fixed at  $\rho_{c(\text{ini})} = 10^{9.95} \text{ g cm}^{-3}$ .

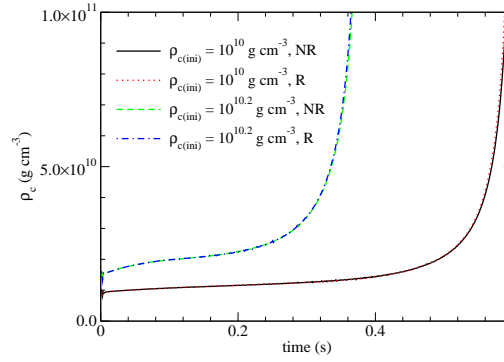


**Fig. 4.** Same as 1, but with or without relativistic corrections. All models are fixed at  $\rho_{c(\text{ini})} = 10^{10}$  and  $10^{10.2} \text{ g cm}^{-3}$ .

In Table 3 we tabulate the results in our simulations. A series consists of models with the same flame structure and input physics, but different initial central densities. For each group, we list the choice of flame structure, the initial flame size, with or without relativistic effects, and the transition density from a direct explosion to a direct collapse. The table can be used to compare directly with models from stellar evolution. For a stellar model with a given runaway mass, its position and its central density, our table can indicate whether this model collapses or not after the ONe deflagration.

**Table 1.** The explode-collapse transition density for our models. Flame stands for the initial flame shape, which includes the centrally ignited kernel (the *c3* flame structure), and off-center kernels (the *b1* and *b5* configuration). See (Reinecke et al., 1999a) for the graphical illustration of these flame structure.  $M_{\text{burn}}$  is the initial mass assumed to be already burnt by deflagration prior to the beginning of simulations. "GR?" stands for the inclusion of relativistic effects in the gravitation potential term.  $\rho_{\text{crit}}$  is the critical density in  $\text{g cm}^{-3}$  above which the models exhibit a direct collapse.

Group	flame	$M_{\text{burn}}$	GR?	$\log_{10}(\rho_{\text{crit}})$
1	c3	$8.6 \times 10^{-4}$	No	9.900
2	c3	$8.6 \times 10^{-4}$	Yes	9.900
3	c3	$6.7 \times 10^{-3}$	No	9.925
4	c3	$4.8 \times 10^{-2}$	No	9.975
5	b1	$1.4 \times 10^{-3}$	No	9.925
6	b1	$2.6 \times 10^{-3}$	No	9.975
7	b1	$2.6 \times 10^{-3}$	Yes	9.975
8	b5	$1.0 \times 10^{-2}$	No	9.975
9	b5	$1.0 \times 10^{-2}$	Yes	9.975

#### 4. Conclusion

In this article we studied the dynamics of the deflagration phase of ONeMg core of the 8-10  $M_{\odot}$  main-sequence stars with different central density, flame structure and input physics. The central density, flame size and its position are important for the final fate of ONeMg. Relativistic effects are less important in comparison. This work shows that the input of stellar evolution is important. Accurate parametrization schemes for the processes before the nuclear runaway takes place, such as convection and semi-convection in the core, are essential for a precise prediction for the final fate of the ONeMg core.

*Acknowledgements.* This work was supported by World Premier International Research Center

Initiative (WPI), and JSPS KAKENHI Grant Numbers JP26400222, JP16H02168, JP17K05382. We thank F. X. Timmes for his open-source subroutines including the Helmholtz equation of state and the torch nuclear reaction network. We also thank M.-C. Chu and L.-M. Lin for the initial inspiration of building the hydrodynamics code.

#### References

- Barth, T. J. & Deconinck, H. 1999, High-Order Methods for Computational Physics (Springer, Berlin), Lecture Notes in Computational Science and Engineering, 9
- Clement, M. 1994, ApJ, 406, 651
- Hashimoto, M., Iwamoto, K., & Nomoto, K. 1993, ApJ, 414, L105
- Jones, S., Roepke, F. K., Pakmor, R., et al. 2016, A&A, 593, 72
- Kim, J., et al. 2012, MNRAS, 424, 830
- Leung, S.-C., Chu, M.-C., & Lin, L.-M. 2015a, ApJ, 812, 110
- Leung, S.-C., Chu, M.-C., & Lin, L.-M. 2015b, MNRAS, 454, 1238
- Leung, S.-C. & Nomoto, K. 2017, JPS Conf. Proc., 14, 020506
- Miyaji, S. & Nomoto, K. 1987, ApJ, 318, 307
- Niemeyer, J. C., Hillebrandt, W., & Woosley, S. E. 1995, ApJ, 452, 979
- Nomoto, K. & Kondo, Y. 1991, ApJ, 367, L19
- Pocheau, A. 1994, Phys. Rev. E, 49, 1109
- Reinecke, M., Hillebrandt, W., & Niemeyer, J. C. 1999a, A&A, 347, 739
- Reinecke, M., et al. 1999b, A&A, 347, 724
- Schmidt, W., Niemeyer, J. C., Hillebrandt, W., & Roepke, F. K. 2006, A&A, 450, 283
- Schwab, J., Podsiadlowski, P., & Rappaport, S. 2010, ApJ, 719, 722
- Timmes, F. X. & Arnett, D. 1999, ApJ, 125, 277
- Timmes, F. X. & Woosley, S. E. 1992, ApJ, 396, 649
- Wang, R. & Spiteri, R. J. 2007, SIAM J. Numer. Anal., 45, 1871